Evaluation of Iodine Compatible Cathode Configurations

IEPC-2019-768

Presented at the 36th International Electric Propulsion Conference
University of Vienna • Vienna, Austria
September 15-20, 2019

Seth J. Thompson[1]
Colorado State University, Fort Collins, CO, 80523, USA

Casey C. Farnell[2] and Shawn C. Farnell[3]
Plasma Controls, LLC, Fort Collins, CO, 80523, USA

Desiree D. Williams[4] and John P. Chandler[5]
Colorado State University, Fort Collins, CO, 80523, USA

and

John D. Williams[6]
Colorado State University, Fort Collins, CO, 80523, USA

Abstract: Iodine is a promising propellant for electric propulsion applications because it can be stored at relatively high density, is easily vaporized and ionized, and compares well with the atomic mass of Xe. Disadvantages of its use include its corrosiveness. This paper describes hollow cathodes and a novel planar cathode configuration that were developed for compatibility with iodine, tested on iodine for durations of a few hours up to 72 hr, and then destructively analyzed. Although made mostly of graphite, both the hollow and planar cathode configurations utilize a new ceramic-metal (cermet) composite insert material that is formed in a one-step heating process from tungsten and BCA-X ceramic powders. In some situations, when operated on iodine, we find that the cermet loses most of its ceramic constituents leaving behind a tungsten foam, which in some situations contains sharp-edged crystalline structures on its surface with nm-level curvature. We speculate that the sharp features may emit electrons via field-enhanced mechanisms. Furthermore, from changes observed in the keeper voltage as a function of time, we also speculate that elevated plasma potentials are established within the insert region as the ceramic material is scrubbed out and the W foam is created. A higher plasma potential within the active zone of the cathode will result in higher fractions of electron emission from volumetric ion generation compared to traditional BCA-W or LaB6 based hollow cathodes. Higher ion generation rates along with the poor thermal conductivity of the W foam will cause the insert to operate conveniently at higher temperatures, where it may be immune to attack by iodine as first demonstrated in research on halide-based, light-bulb technology. In addition to test results and destructive analysis observations, we present a discussion of future work we are planning that may elucidate our currently speculative understanding of hollow cathode operation on iodine.

[1] Graduate Research Assistant, Department of Mechanical Engineering, Seth.Thompson9@gmail.com
[2] Research Engineer, Casey.Farnell@plasmacontrols.com
[3] Research Engineer, Shawn.Farnell@plasmacontrols.com
[4] Research Associate, Department of Mechanical Engineering
[5] Research Associate, Department of Mechanical Engineering
[6] Professor, Department of Mechanical Engineering; and Technical Director, Plasma Controls, LLC, drjohndarrylwilliams@gmail.com

I. Introduction

Some Hall effect thruster (HET) propulsion systems utilize xenon gas as a propellant, which is expensive and must be stored in heavy, high-pressure tanks. Even in high-pressure propellant tanks, the maximum density of xenon is only twice that of liquid water, and lower than many condensable propellants. Krypton is less expensive, but its maximum density is lower than xenon leading to even larger, high-pressure tanks. Iodine (I_2) is an alternative propellant with the potential to overcome some drawbacks of xenon and krypton through its lower cost, higher storage density, and greatly decreased tank pressure. Hall effect thrusters from several hundred watts up to ten kilowatts have been demonstrated using iodine propellant, with performance comparable to that of HETs operated on xenon[1,2]. As typical of any new propellant it is difficult to address all challenges at once, and, as a result, much of the iodine thruster testing was performed with hollow cathodes operated on xenon or other inert gases. Due to the reactive nature of iodine, it is difficult to operate traditional hollow cathodes on iodine propellant for more than tens of hours. Although there are reports of cathodes running on iodine for short periods, these cathodes have not been able to operate consistently enough to test with iodine thrusters[3,4].

Our recent work has focused on developing an iodine compatible hollow cathode that uses a tungsten insert formed from a ceramic-metal composite (cermet) precursor insert, which is operated on iodine for some time to scrub out the ceramic and leave behind a free-standing, open-pore tungsten foam. The foam characteristics are determined to some extent by the initial size and relative quantity of tungsten powder used in the cermet and a self-assembly process that presently isn't well understood. There is little knowledge of the material interactions that occur between surfaces and partially ionized iodine gas at temperatures of 600 K to 1650 K that are typically encountered inside hollow cathodes. The goal of our effort is to develop a hollow cathode capable of operating stably on iodine for thousands of hours. To avoid time-consuming life tests, shorter duration tests have been conducted on cathode prototypes to analyze the effects on internal surfaces and quantify corrosion rates and related issues that may limit lifetime. This paper summarizes our efforts to date on this work, with Section II containing some background information on hollow cathodes used in electric propulsion and the reasoning behind selecting certain materials to be used with iodine guided by research on halide use in light bulbs. Section III provides descriptions of our methods and materials, and Section IV presents results and discussion. Finally, in Section V, we summarize our findings and make recommendations for future work.

II. Background

Hollow cathodes are used in HETs as a plasma electron source to initiate the main plasma discharge inside the channel and to neutralize the beam of ions produced by the thruster.[5] Traditional hollow cathodes typically consist of a refractory metal tube such as tantalum, molybdenum, molybdenum-rhenium with a tungsten or Mo-Re orifice plate welded to the end. A low-work function insert is placed inside the refractory tube at the downstream end near the orifice plate. Common inserts are formed from porous tungsten impregnated with materials such as barium calcium aluminate that is formed from barium oxide BaO, calcium oxide CaO, and aluminum oxide Al_2O_3 (designated BCA in ceramic materials nomenclature); lanthanum hexaboride LaB_6[6]; or BCA-scandate.[7] Once heated, the insert will thermionically emit electrons that are subsequently extracted to the anode or ion beam. A heater is often used to raise the cathode and insert to thermionic emission temperatures before starting, but this is not strictly necessary as hollow cathodes can be started without a heater. The temperature of the cathode tube varies with distance from the orifice plate, with the highest temperature located at the orifice and decreasing temperature as heat is conducted upstream along the tube. As a result, the cathode tube and insert temperatures may vary from less than 600K to nearly 1650K depending on the insert type, orifice geometry, and operating conditions, such as emission current, flow rate, and the type of low work function material used.

A literature survey of the chemical reactivity of iodine with several materials, suitable for cathode components, at moderate temperatures below 450 °C was reported by Polzin et al.[8] To our knowledge, there is little or no information of material interactions that occur at elevated temperatures of 1250 K to 1600 K in the presence of plasma that exists near the cathode tip. One source of information on the effects of high temperature with iodine comes from the development efforts of quartz-halogen lamps performed throughout the 1950s and 1960s. Iodine was introduced into these lamps to increase tungsten filament life through the formation of a chemical life cycle between tungsten and iodine. Specifically, the iodine vapor concentration in the lamp is set to a value where it reacts with tungsten deposited on the bulb surface as fast as the tungsten sublimes off the filament and deposits onto the bulb. At the bulb surface temperature, the iodine atoms react with the deposited tungsten to form gaseous WI_2 effectively scrubbing the bulb clean. In addition, the WI_2 gas molecules eventually collide with the tungsten filament

where the filament, at temperatures near 2500℃, would cause the WI_2 compound to dissociate and deposit the tungsten back onto the filament and release the iodine to repeat the process.[9] In this way, the tungsten filament lifetime was extended, and the bulb surface of the lamp was kept clean. Molybdenum, tungsten, and platinum were often used in support structures to minimize corrosion by iodine. In later years graphite was used to form the support structures to further reduce iodine interactions at elevated temperatures (~1000℃) and to act as an oxygen getter to combat the water cycle that can form and limit the lifetime of the lamps.[10] This lamp development work has served as our guide for selecting potential cathode component materials and for uncovering strategies that might enable the creation of hollow cathodes that are compatible with iodine vapor at elevated temperatures.

III. Methods and Materials

A. Iodine Feed System

For laboratory testing, an iodine vapor feed system was constructed. Dedicated PID controllers were used to control the temperature of the in-vacuum feed lines, airside feed lines, and the iodine reservoir where 99.9% pure I_2 crystals are stored before starting a test. An in-line, flow-limiting orifice was used in combination with the reservoir temperature to adjust the flow rate of iodine. The reservoir temperature was adjusted between 65℃-85℃ depending on the desired flow rate. The remainder of the feed system, including the flow-limiting orifice, was held around 40°C higher than the reservoir to avoid condensation of iodine vapor on feed lines and components. A total of ten thermocouples were monitored along the feed system to record and control temperature across all feed system components. Finally, the flow rate is measured independently by weighing the iodine reservoir before and after

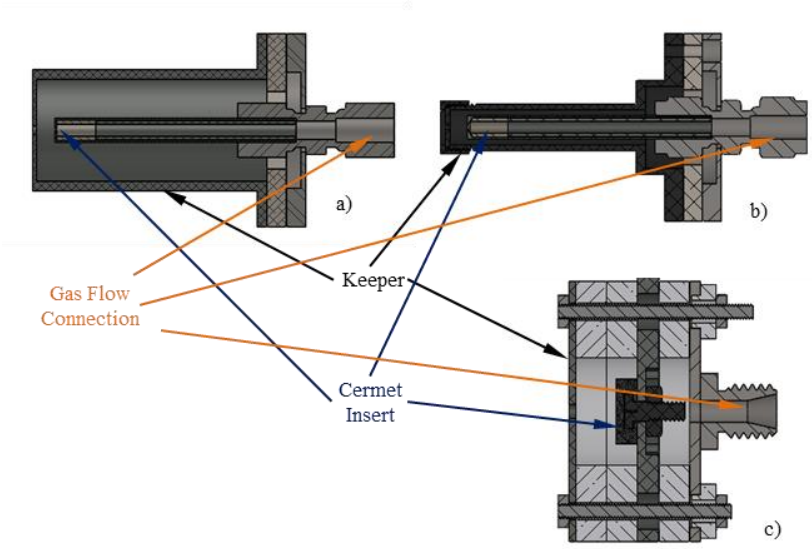

Figure 1. Cross-sections of cathode configurations tested. The cathodes shown in a) and b) are traditional tubular hollow cathodes with enclosed keepers; while the cathode shown in c) is a planar cathode configuration. In all three cathodes, the gas enters the assembly on the right and flows to the downstream keeper orifice on the left.

B. Cathodes

As discussed previously, two top candidates for iodine compatible cathode materials are tungsten and graphite due to their successful integration into halogen lamps. The one important difference between our approach and the one used in halogen lamps is that we hope to control the temperature of the W foam insert to be hot enough to eliminate the concern for attack by iodine, but not hot enough to limit the life of the insert due to evaporation processes. Two cathode configurations were developed that utilize graphite as the primary material in contact with the precursor cermet inserts and iodine vapor. Cross-section sketches of the cathode assemblies tested are shown in Fig. 1, with Figs. 1a and 1b representing the traditional tubular hollow cathode configurations utilizing a graphite cathode tube and keeper. The smaller gap between the cathode and keeper tubes in Fig. 1b relative to the gap between the cathode and keeper orifices was selected to determine the effects of these changes on starting characteristics relative to the geometry used in Fig. 1a following work by Ham et al.[11] Although not used in this study, the structure at the tip of the keeper in Fig. 1b allows one to replace the keeper orifice plate to investigate the effects its geometry has on starting characteristics and steady state operation. Thin, tubular graphite liners are used to hold the cermet insert in place in tubular cathode configurations based on Figs. 1a and 1b.

Figure 1c shows a cross-section of a planar cathode configuration with the cermet insert attached to a graphite plate held at cathode potential. This configuration has been used on argon and krypton[12] with a Ta plate and Ta foil

to hold the insert. All graphite components shown in black in Fig. 1 are made of EDM-3 graphite, while all lighter components are made of alumina silicate. The cathode arc is coupled to an anode, which is formed from a flat graphite plate that is 10 cm in diameter and located 2-cm downstream of the keeper electrode to simulate the operation of a HET or ion thruster.

C. Measurements

Anode and keeper currents and voltages were recorded during the operation of cathodes on argon and iodine as changes in coupling voltages are expected to occur when iodine reacts with and removes the ceramic material contained within the cermet insert. In fact the voltages are observed to rise with time, and we believe that, as the ceramic material is removed from the insert, the keeper and anode voltages rise to maintain the discharge with an insert that has a higher effective work function. We also believe that the plasma potential inside the cathodes near the W foam inserts will rise with time and cause the fraction of electron emission due to ion generation (relative to thermionic emission) to also rise. Cathodes were dissected for visual inspection and subsequent material analysis after operating on iodine using a scanning electron microscope (SEM) to examine the micro-features of the insert while energy-dispersive x-ray spectroscopy (EDS) was used to determine changes to the material composition of the insert after operation on iodine. Straight forward imaging of the insert surface was performed in addition to imaging of the interior of the insert after cross-sectioning and ion beam polishing it.

D. Vacuum test facility

A test facility was constructed at CSU to evaluate hollow cathodes on iodine vapor. The system utilizes a 4-inch diffusion pump with a pumping speed of ~200 l/s on Ar. A polycold mated to a cold trap was used to cool the trap to condense iodine during testing. After testing was complete, the cold trap was warmed to sufficient temperatures to vaporize iodine for subsequent removal. The vacuum chamber was lined with sacrificial aluminum foil that reacts with the iodine vapor, protecting the stainless-steel walls from corrosion. This foil was replaced after each cathode test. The mechanical pump is protected by an activated charcoal trap to limit iodine exposure to corrodible surfaces within the pump. The chamber is sealed during the venting while air is circulating through the chamber to remove any remaining iodine vapor to a safe location. The test facility interlock system has been upgraded to prepare for longer-term, automated testing of cathodes. The interlock upgrades have caused some tests to stop, and vacuum components have failed causing other tests to be stopped. Although undesirable, we took advantage of the different test durations by destructively analyzing cathodes and inserts to gain an understanding of how iodine affects these components as a function of testing time. The results of the tests and observations from the destructive analysis are described in the next session.

IV. Results and Discussion

We report data collected on four tubular hollow cathodes and one planar cathode, which were all first operated on Ar for a few hours prior to being operated on iodine vapor for periods of time ranging from 6.7 to 72 hr. As indicated in Table 1, of the four tubular hollow cathodes operated on iodine vapor, only one test was voluntarily terminated, denoted Tubular 1 in the table. The other tests were terminated due to a variety of test facility malfunctions. Figure 2 shows photographs of one tubular cathode tip prior to testing and three tubular tips after operation on argon and iodine. The erosion of the graphite cathode orifice plate was caused by starting on Ar. The following paragraphs present testing details in greater detail along with changes to the cermet inserts observed after operation on iodine.

A. Tubular Hollow Cathode Test Results

Each of the cathodes listed in Table 1was first operated on argon gas for a several hours prior to introducing iodine vapor. Cathodes were started on argon in a heaterless fashion, meaning no heater was used to bring the cermet insert to thermionic emission temperatures prior to operation,[11] and operation on Ar allowed us to warm the entire cathode assembly, which prevented iodine condensation on cathode components that would have occurred if the cathode were started from a cold state on iodine. The pre-test operation on Ar also allowed us to ensure the cathodes were operating normally prior to operation on iodine.

Table 1: Summary of cathode testing on iodine (I_2)

Cathode	Operation Time	Keeper Voltage	Anode Voltage	Keeper Current	Anode Current	Flow Rate ($\dot{m}$)	Termination of Test
Tubular 1	72 hrs	18 V	35 V	3.0 A	5.0 A	4.0 sccm - 0.76mg/s	Voluntary
Tubular 2	6.7 hrs	24 V	37 V	1.0 A	5.0 A	(3.2) sccm - (0.6) mg/s	Facility Malfunc.
Tubular 3	25.4 hrs	27 V	39 V	1.0 A	5.0 A	4.3 sccm - 0.81 mg/s	Facility Malfunc.
Tubular 4	22.1 hrs	18 V	32 V	1.0 A	5.0 A	2.1 sccm - 0.4 mg/s	Facility Malfunc.
Planar	17.3 hrs	21 V	48 V	1.0 A	3.5 A	1.6 sccm - 0.31 mg/s	Facility Malfunc.

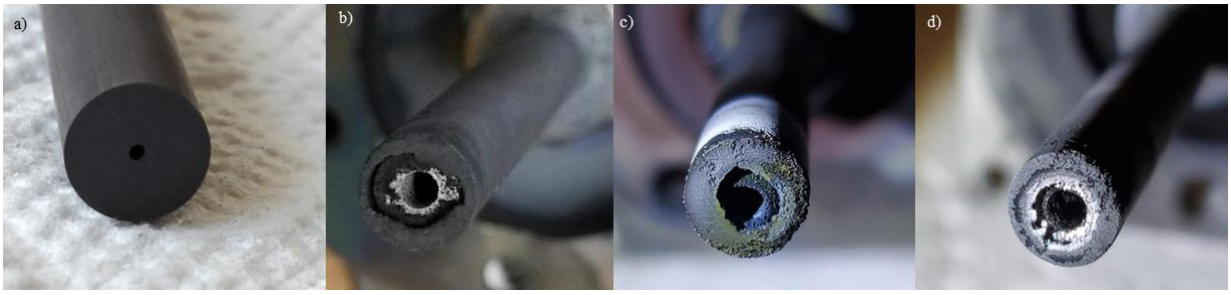

Figure 2. Photographs of graphite cathode tubes and orifices pre- (a) and post- (b-d) operation.

The Tubular 1 test was the longest operation of a cathode on iodine in our testing conducted to date. This test was 72 hours in duration and was voluntarily terminated for destructive analysis of the cathode components and insert. The cathode utilized a graphite cathode tube, with a graphite liner to hold the insert near the orifice plate end of the tube. The cathode was operated at a flow rate of ~4.0 sccm (I_2) at a total emission current of 8.2 A (keeper and anode current combined). This flow rate is ~13% of the anode flow rate for a typical HET operated at an anode current of 8.2 A, which is only slightly higher than the commonly accepted ~10% flow ratio used in many laboratory and flight HETs. After operation on iodine the graphite cathode tube and insert were cross-sectioned, and the tube wall thickness measured at several locations ranging from near the cathode orifice to the upstream location near the cathode baseplate. No measurable (<10 μm) change in graphite cathode tube wall thickness was observed.

The test of Tubular 2 was terminated as a result of a view port cracking leading to a loss in vacuum. As a result of the failure, the feedlines may have cooled unevenly and flow may not have ceased when the cathode discharge was extinguished. This could lead to inaccuracies in the flow rate measured by averaging the mass loss of the reservoir before and after operation on iodine. This possible inaccuracy in flowrate measurement is represented by parenthesis around the value reported in the table. The test of Tubular 3 was ended as a result of the vacuum chamber pressure rising above a level that caused the interlock system to trip. This cathode utilized a cermet insert with twice the weight percentage of tungsten used in the cermet inserts for all other tests. This difference in insert composition may have contributed to the higher keeper and anode voltages. The test of Tubular 4 was ended as a result of loss of water cooling to the pump train, which caused an interlock to trip. This cathode was operated at a much lower iodine flow rate with lower keeper and anode voltages, and very good voltage stability.

A troubling result with all tubular hollow cathode tests conducted is the significant orifice damage that was observed after the tests were stopped. Figure 2a shows a photograph of a graphite cathode tube orifice prior to testing and photographs in Figs. 2b through 2d show cathode tips after testing. Further investigation revealed that the cathode orifice damage occurred as a result of heaterless starting and was observed after starting and operating on argon. We are currently working on an improved soft-start circuit and modifying the cathode-keeper geometry and materials to prevent this damage from occurring. Although the planar cathode test reported upon in the following section did not experience arcing damage, we have tested additional prototype cathodes where some arcing damage

was observed. One possible fix to the problem of arcing that damages the graphite components held at cathode potential is to use shaping of the tungsten-based cermet to (1) create the cathode orifice feature and (2) shadow the graphite surfaces. This is possible because the cermet inserts can be cast into nearly any shape similar to how powder cast parts are manufactured in injection molding processes.

B. Planar Cathode Test Results

A similar test to the ones conducted on the tubular cathodes was performed with the planar cathode shown in the sketch in Fig. 1c. This cathode was operated on iodine for a total of 17 hours before a facility power failure caused an early termination of the test. The cathode operated in a very stable mode at a low flow rate of 0.3 mg/s with keeper voltages similar to that of the tubular cathode tests. Specifically, the keeper voltage stabilized at ~20V, however, the anode voltage was higher at ~45V. at a total emission current of ~4.5A. The anode voltage was higher for the planar cathode test, which might have been due to build on contamination on the anode plate.

A shift in voltages was observed after ~3 hours of operation on iodine with the planar cathode. We believe this to be the operational time when the majority of the ceramic had been removed from the insert by iodine, which was our conclusion related to a similar shift in voltages at ~3 hr observed in the 72-hour test conducted on the tubular cathode. The graphite plate used to attach the cermet insert in the planar cathode showed little to no degradation after the 17-hour test as expected. After the test, the insert was removed from the cathode assembly for analysis in the SEM.

C. Insert changes

The following sections discuss the changes that were observed in the cermets used in the iodine testing. We start by discussing the planar cathode and its cermet, and then we discuss the tubular cathodes after first showing what a typical cermet looks like after operation on Ar for 72 hr.

1. Details related to planar cathode analysis

Figure 3 contains a sketch and photograph of the planar cathode. The cermet used in this cathode was a squat right cylinder that was placed in a Ta foil cup that was then attached to a graphite mounting plate using a high temperature graphite paste. The graphite mounting plate was machined to be very thin in the region where the cermet is attached to limit the heat flow from the cermet to the graphite and cathode assembly.

Figure 4 contains photographs of the cermet insert mounted to the graphite plate after it was tested on iodine and mounted on an SEM fixture next to an un-operated cermet. The un-operated cermet appears dark because of the microscopic texturization of its surface, which is revealed in the higher magnification SEM images shown on the left hand side of Figure 5. The operation on iodine causes the surface texture to be much smoother, but it doesn't appear to change the insert much in a macroscopic sense. The Ta foil used to hold the cermet to the graphite mounting plate, however, is shown to be eroded by the exposure to dense iodine plasma, which isn't unexpected because the Ta foil is very thin and Ta is reactive with iodine as found in research on halide-based lamps in the 1950's. We did not cross section the planar inserts, and hence could not gather compositional data versus depth from the emitting surface using the SEM-EDS tool, however, we plan to do this with cermets tested in planar cathodes in the future. Although there appears to be a depression in the planar cermet shown in Figure 13 that was operated on iodine, the same depression is present in the un-operated cermet as this feature is caused during the cermet fabrication process.

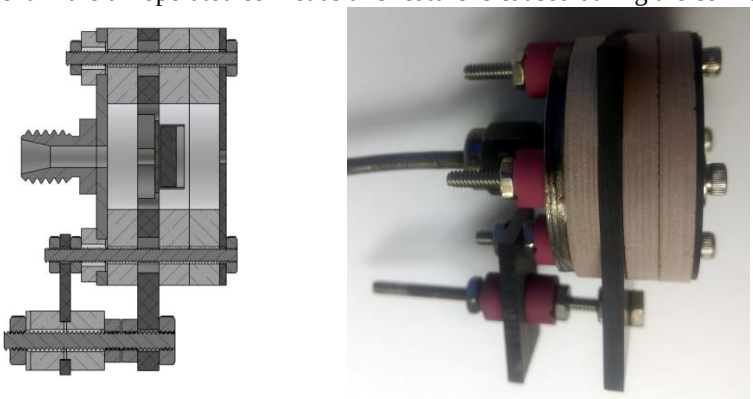

Fig. 3. Planar cathode sketch and photograph.

(a) (b)

Fig. 4. Photograph of cermet insert on graphite mounting plate after removing keeper plate (a) and photograph of cermets un-operated, left, and operated, right, (b) prior to being placed in the SEM for imaging. Note that the dark coloring of the un-operated cermet is due to the microscopic texture of the cermet that results in a high absorption coefficient and not due to oxidation in the formation process. The operation on iodine caused the surface texture to become smoother as shown below in SEM images in Fig. 5.

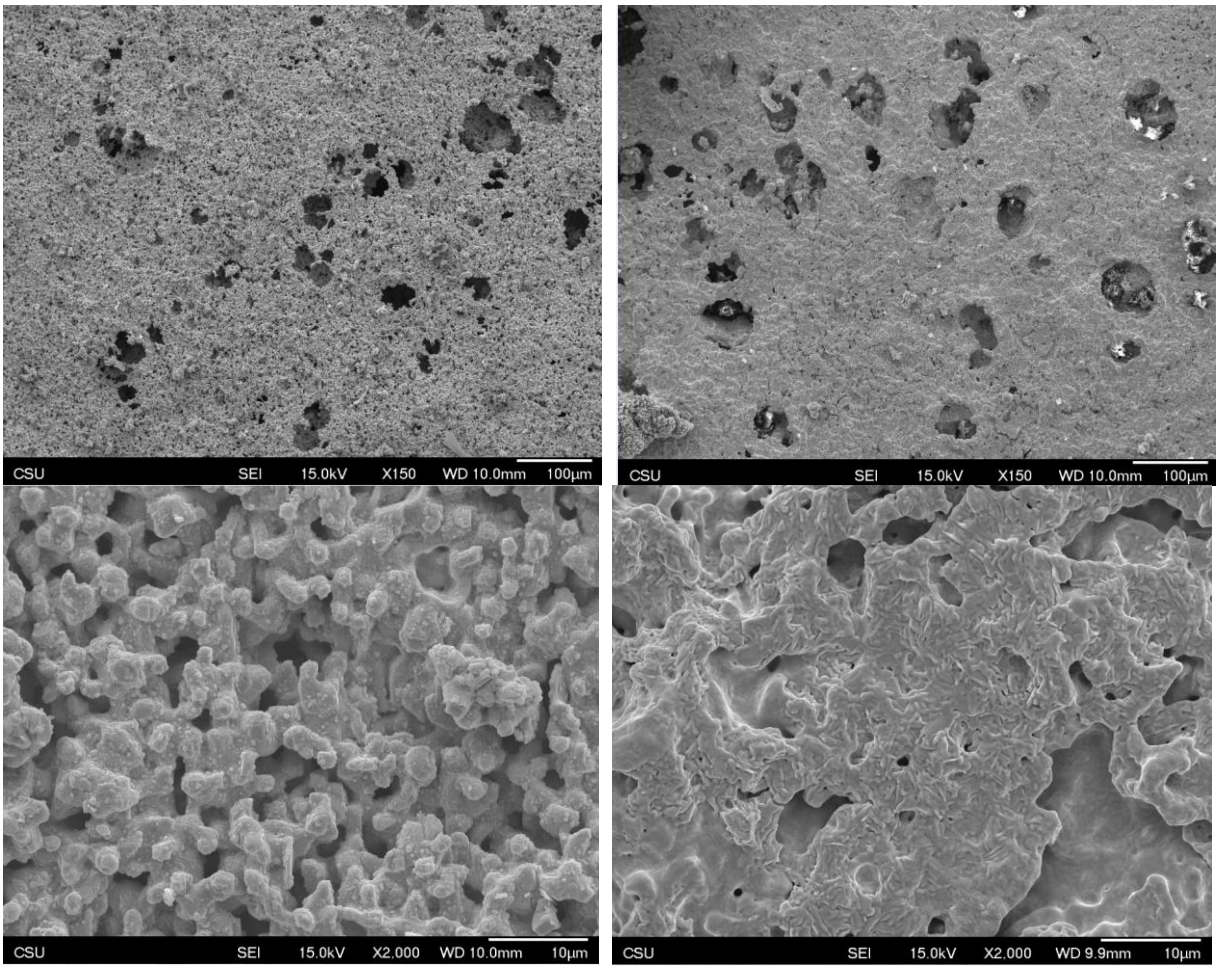

(a) (b)

Fig. 5. SEM images of planar cermets un-operated (a) and after operation on iodine (b) at different magnifications. The course porosity of the original cermet fabrication process is preserved (see low mag images in top row), but the fine texturization is modified after operation on iodine to be much smoother (see higher mag images in bottom row).

2. Tubular 2 Insert Changes

We will discuss the analysis of Tubular 2, 3, and 4 inserts prior to discussing the Tubular 1 insert, but, before discussing the changes observed in the Tubular 2 cathode operated on iodine, it is instructive to look at a cermet that was only operated on Ar in a Ta tube, like the one shown in the photograph in Figure 6. The Ta tube has an orifice at its downstream end that was formed directly from the 6.4 mm diameter Ta tube material using a rolling operation. After testing on Ar for 72 hours the Ta cathode was cut open, and then its cermet insert was cross sectioned and ion beam polished. The insert is shown in an SEM image in Figure 7. We note that the weight ratio of W powder used in the fabrication of this insert was 5:1 relative to the weight of the BCA ceramic powder, which is similar to the weight ratios of the cermets used in Tubular 1, 2, and 4 cathodeds in Table 1.The cermet insert used in the Tubular 3 cathode was fabricated with a weight ratio of 10:1.

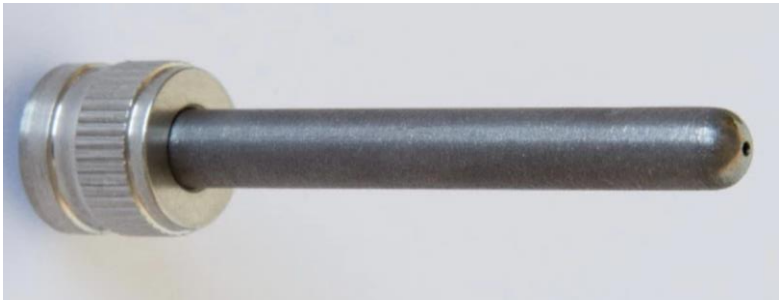

Figure 6. Photograph of a Ta cathode designed for operation on inert gases.

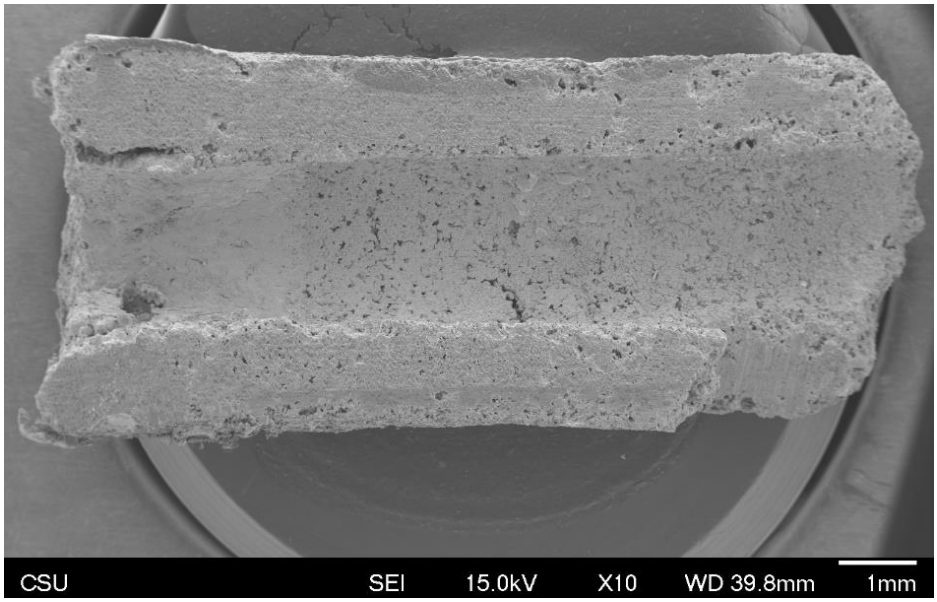

Upstream End Tip End

Figure 7. Cross-sectioned, tubular cermet insert from a Ta cathode operated on Ar for 72 hr after the cross-sectioned region was ion polished. A chip was unintentionally formed at the tip end (shown in the bottom right corner of the photograph).

The SEM was used to zoom in on several locations on the polished wall of the insert, and SEM images using the SEI and Compo viewing modes are shown in Figures 8 and 9 at 500X mag at an axial location (measured from the tip) of 0.5 and 1.0 mm and a radial location midway between the inner and outer diameter. The SEI images show the general surface to be similar in the two locations, and the Compo (short for compositional) images show a tungsten (lighter region) matrix that is completely infiltrated with ceramic material (darker regions comprised of barium calcium aluminate-- BCA). The ceramic material isn't completely of one uniform phase, but instead is mottled with lighter and darker regions that indicate the presence of several phases. This occurs because some

scandate is used in the BCA ceramic material, and it substitutes for some of the alumina constituent, which creates a mottled appearance because scandium has a higher atomic number compared to aluminum. It is also pointed out that some of the calcium oxide constituent doesn't completely react with the other constituents of the BCA impregnant, and the isolated CaO material can appear darker in Compo images compared to the fully reacted BCA material. We also point out that the ceramic material at the 0.5 mm axial location is not as dense as the material at 1.0 mm due to the cermet insert formation process. The large reserve of barium containing material located further upstream in the cermet is believed to be readily available as needed to keep the insert running at nominal conditions. In addition to SEI and Compo studies, we performed a more detailed compositional study using the EDS tool included in the CSU SEM. A composite image was formed from the EDS data collected at the 1.0 mm location and it is shown in Figure 10. The barium constituent is shown to be fairly uniformly distributed throughout the ceramic regions while the calcium oxide and alumina constituents are more localized.

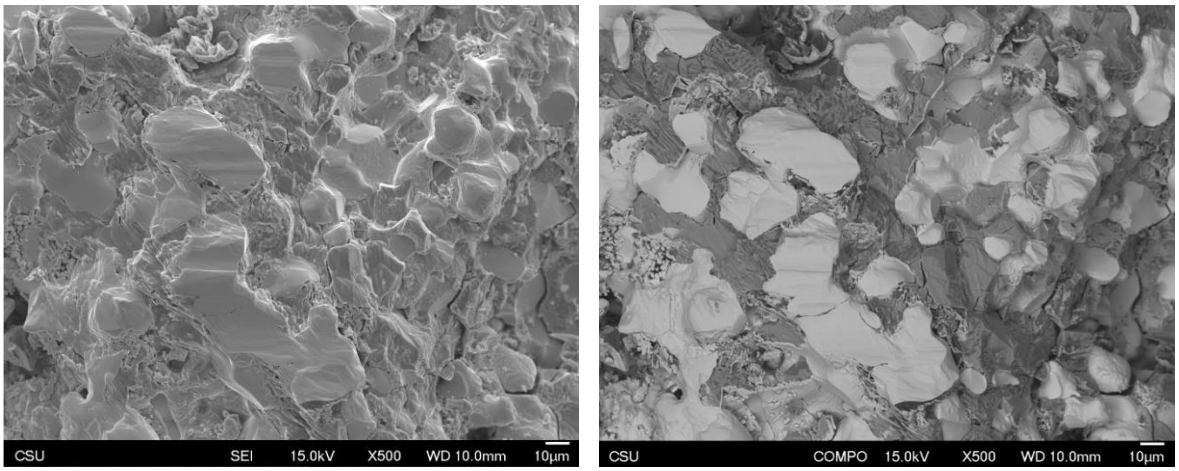

Fig. 8. SEI and COMPO images of an insert from a Ta cathode operated on Ar for 72 hr at an axial location of 0.5mm from the insert tip and a radial location midway through the insert wall thickness.

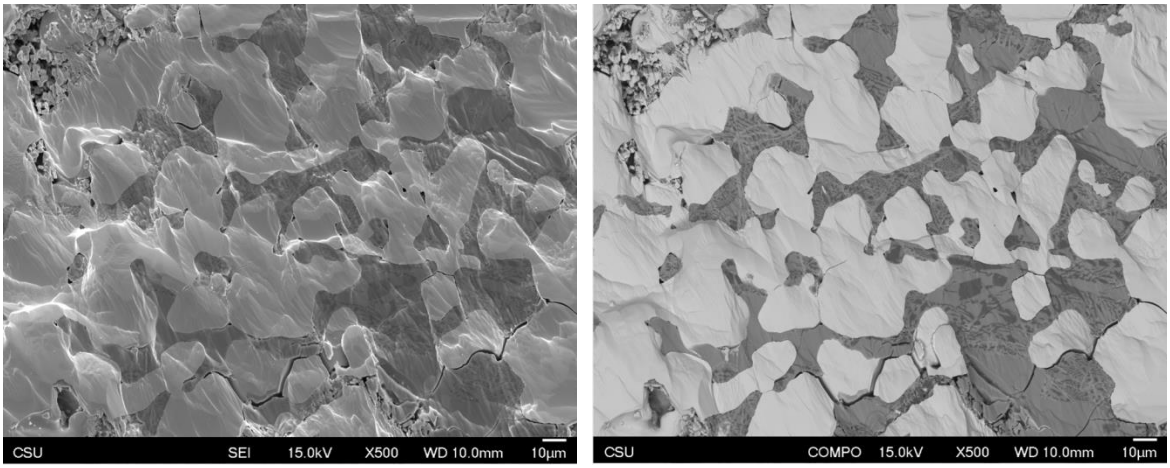

Fig. 9. SEI and COMPO images of an insert from a Ta cathode operated on Ar for 72 hr taken at an axial location of 1.0 mm from the insert tip and a radial location mid way through the insert wall thickness.

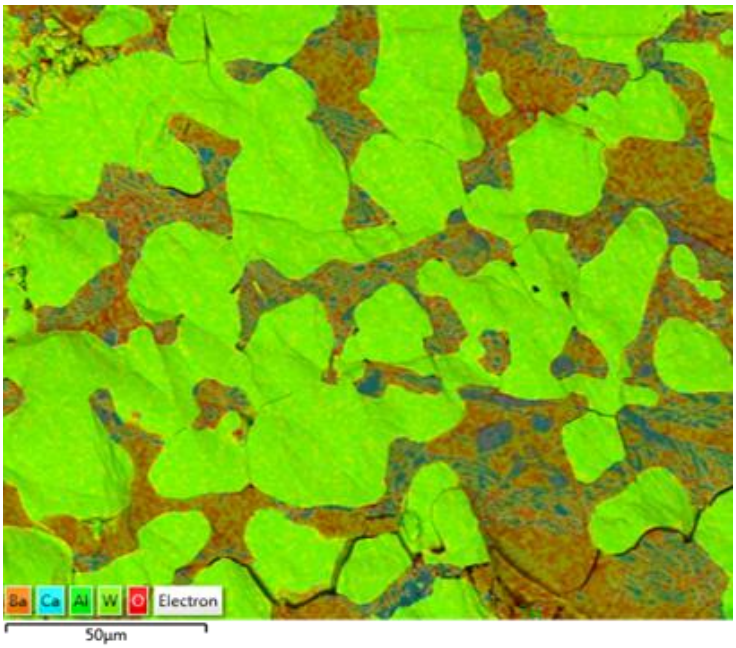

Fig. 10. Combined compositional EDS data for an insert from a Ta cathode operated on Ar for 72 h at an axial location of 1.0 mm from the insert tip and a radial location mid way through the insert wall thickness.

Next we will present the analysis of the cermet insert from the Tubular 2 cathode. As mentioned above, the Tubular 2 cathode used a cermet insert that was fabricated with a W to BCA weight ratio of 5:1. A sketch of the cathode assembly along with photographs of the cathode tip region before and after testing are shown in Figure 11. A glass window port cracked after testing the cathode on iodine for 6.7 hr. The cracked window vented the chamber while the cathode was being operated, and an interlock stopped the test. Although most of the subsystems were switched off, the keeper power supply and iodine flowrate were not. The keeper and anode discharges extinguished, and the keeper power supply voltage rose, which caused additional arcing until the power supply was switched off several minutes after the window cracked. The post-test photograph of the cathode tip indicated that arcing damage occurred to the graphite orifice plate. This wasn't unexpected because graphite is known to be easily damaged by cathodic arcs, but we weren't certain if the damage occurred before or after the window cracked and if starting the cathode on Ar or Iodine caused damage. We did detect arcing during starting of the Tubular 2 cathode on Ar, and subsequent testing on the Tubular 3 and 4 cathodes indicated that the erosion of the graphite tip region was due to cathodic arcs that occurred during startup when using Ar gas.

An SEM image of the cross-sectioned cermet insert from the tubular 2 insert is shown in Fig. 12. Although the hot cermet insert was exposed to air after the window crack, it does not appear to be severely affected by the exposure. Figure 13 contains a higher magnification SEM image of the tip region of the cermet. This image is of the ion beam polished, cross-sectioned wall, and three circles are drawn on the image that indicate where additional, higher magnification images were collected. The first thing we'd like to point out is the highly porous nature of the cermet material that is revealed in Figure 13 that is much different than the cermet operated only on Ar. The iodine appears to scrub out quite a bit of the ceramic component of the cermet in 6.7 hr, and this will vastly diminish the heat conduction, allowing the insert to become hotter under similar plasma conditions compared to a cermet with the ceramic constituent present (see Fig. 9 for example).

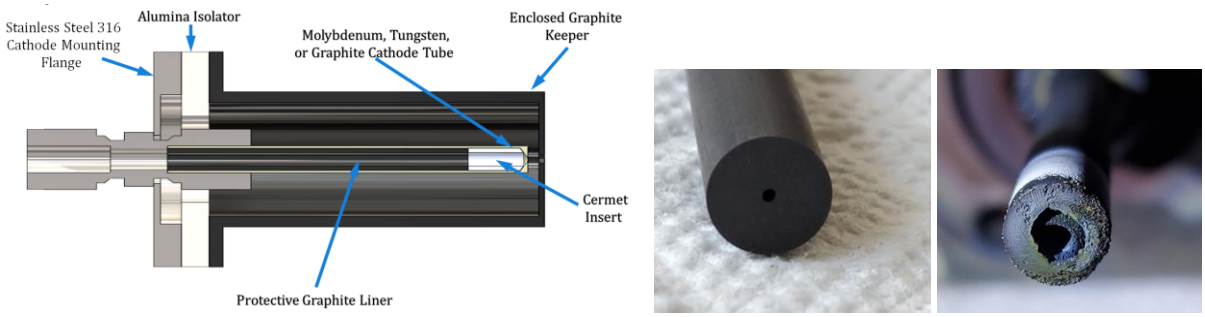

Fig. 11. Tubular graphite cathode design (left) used to evaluate the Tubular 2 cathode, and a photograph of the cathode tube tip region taken before (middle) and after (right) testing. The erosion of the cathode orifice plate was due to arcing during start up on Ar. The cathode was operated on Ar for 1.7 hr and iodine for 6.7 hr before a glass window port cracked and vented the chamber.

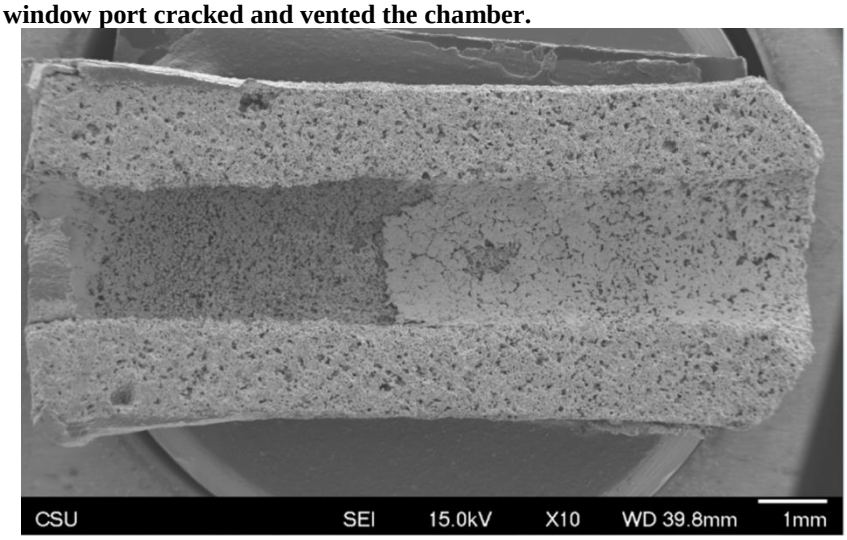

Fig. 12. SEM image of the Tubular 2 cermet insert taken after cross sectioning and ion beam polishing.

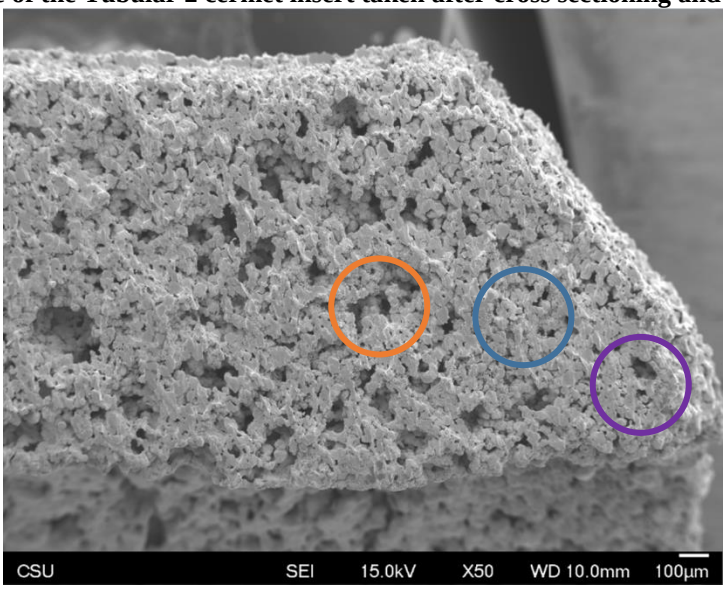

Fig. 13. Higher magnification SEM image of the tip region of the Tubular 2 cermet insert taken after cross sectioning and ion beam polishing. Colored circles indicate approximate locations where additional data were collected.

The higher magnification SEM (SEI and Compo) images contained in Figures 14-17 and the layered EDS image contained in Figure 18 reveal additional information about the Tubular 2 cermet insert at axial locations of ~0.25, 0.5, and 1.0 mm (measured from the tip). The Compo images are useful for quickly determining regions where different materials exist, and the images in Figure 14 (Compos on right side) taken 0.5 mm from the tip indicate that mostly tungsten is present with open pores between the tungsten matrix. A smaller amount of ceramic at the 0.5 mm axial location was observed as contrasted with the cermet images shown in Figs. 8 and 9 that were collected after operation on only Ar. Images taken at the 0.25 mm axial location on the Tubular 2 insert are shown in Fig. 15, and they appear similar to the 0.5 mm images except that more ceramic is present.

Figures 16 and 17 show images taken at an axial location of 1.0 mm, and the high magnification images in Fig. 17 indicate more clearly the presence of some ceramic. The EDS tool was used to identify the composition of the ceramic, and these data are shown in the layered EDS images in Fig. 18. The only ceramic constituent detected was scandium oxide, and informal discussions with Wayne Ohlinger at the Energy and Propulsion Forum in Indianapolis, Aug. 2019, revealed that this result is consistent with the difficulty that iodine has in reducing scandium oxide relative to the ease in which it can reduce barium oxide, calcium oxide, and alumina. The only mystery is why more scandium oxide is present at 0.25 mm and 1.0 mm and less exists at the 0.5 mm location. One explanation is that the scandium oxide is being melted near the 0.5 mm position and wicked toward the hotter tip end of the insert, but not being melted at the 1.0 mm.

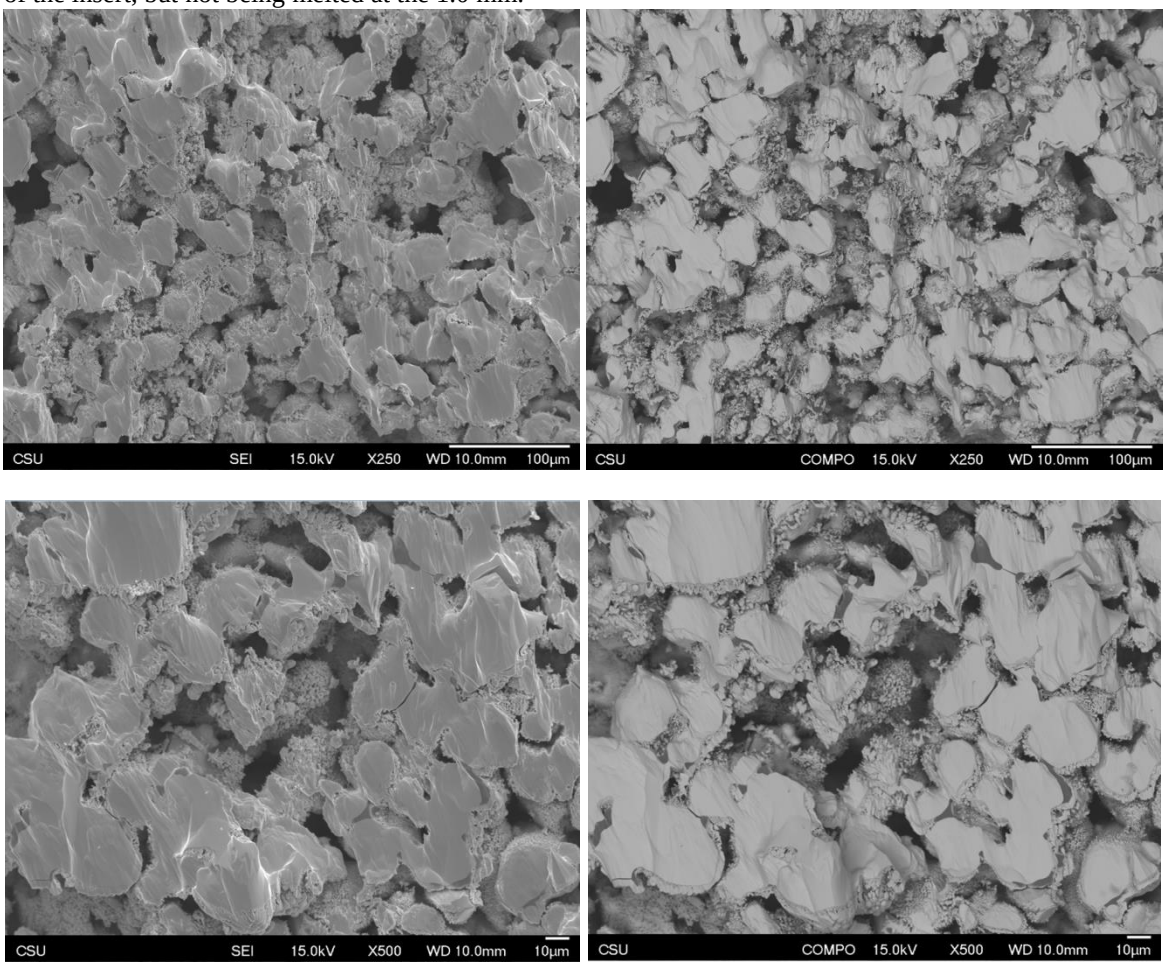

Fig. 14. SEM SEI and Compo images of the tip region of the Tubular 2 cermet insert at an axial location 0.5 mm from the tip and a radial location midway between the inner and outer diameter.

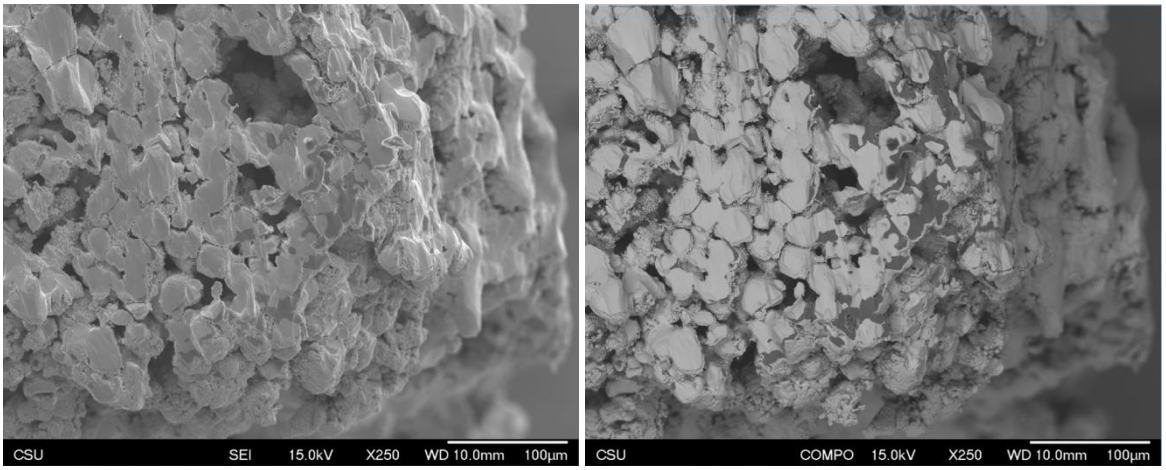

Fig. 15. SEM SEI and Compo images of the tip region of the Tubular 2 cermet insert at an axial location 0.25 mm from the tip and a radial location on the cross-sectioned wall near the inner diameter.

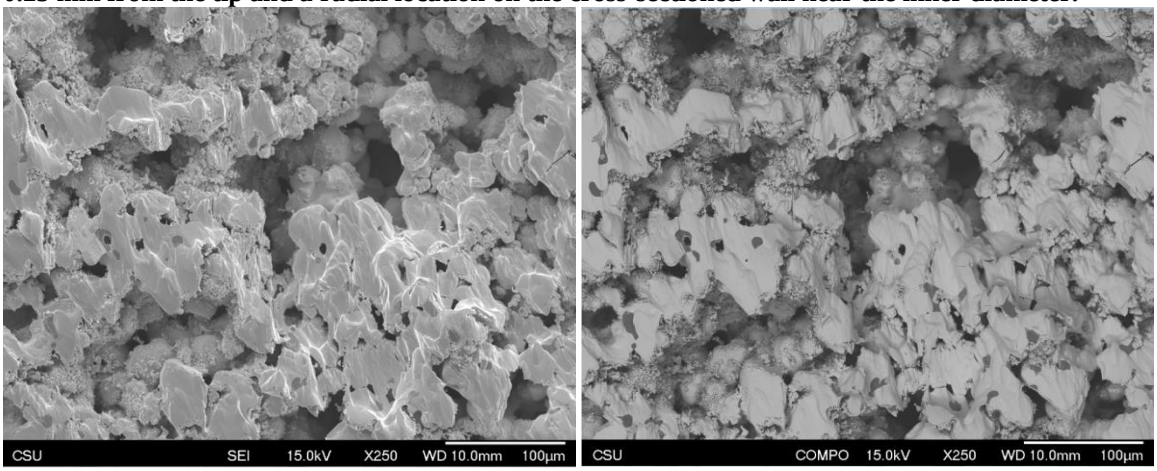

Fig. 16. SEM SEI and Compo images of the tip region of the Tubular 2 cermet insert at an axial location 1.0 mm from the tip and a radial location on the wall midway between the inner and outer diameter.

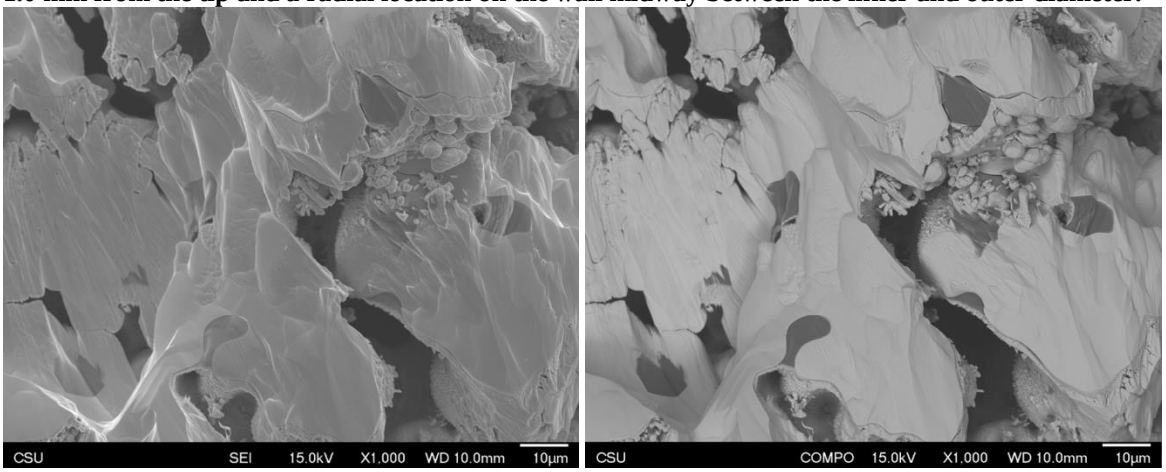

Fig. 17. Higher magnification SEM SEI and Compo images of the tip region of the Tubular 2 cermet insert at an axial location 1.0 mm from the tip and a radial location on the wall midway between the inner and outer diameter of the insert.

(a) (b) (c)

Fig. 18. EDS layered images taken at axial locations 1.0 mm (a), 0.5 mm (b), and 0.25 mm (c) from the tip of the Tubular 2 insert.

3. Details related to Tubular 3 cathode analysis

As mentioned above, the Tubular 3 cathode used a tubular cermet insert that was fabricated with a W to BCA weight ratio of 10:1, which is more W compared to the other cermets in this paper. Photographs of the cathode tip region and the cermet insert after testing are shown in Fig. 19. A vacuum pressure spike caused the interlock system to shut the test down after ~25-hr of testing on iodine at a flow of 4 sccm I_2. At this point, the cermet insert was removed from the graphite tube, cross-sectioned, ion polished, and imaged in the SEM (see images in Figs. 20 and 21). One interesting feature of the Tubular 3 cermet is the relatively porous state of the interior relative to the Tubular 2 cermet, which is counter intuitive because, as mentioned, the starting concentration of W is higher in the Tubular 3 cermet. Conversely and as expected, the Tubular 3 cermet doesn't appear to have as much (if any) ceramic left in its interior at the 0.5 mm location. It is possible that the BCA constituents were scrubbed out by iodine and the Sc_2O_3 constituent was melted and wicked out toward the hot surface at the inner diameter near the tip, vaporized at this inside surface, and carried out of the cathode. Although this explanation seems plausible, data from the Tubular 4 cathode testing contradicts this conclusion as discussed in the next section.

Fig. 19. Photograph of the graphite cathode tip (left) of the Tubular 3 cathode after testing on Ar and iodine for 2.3 hr and 25 hr, respectively. Damage to tip was very likely caused by arcing during starting on Ar. Photograph of the downstream end of the cermet insert (right) after removal from the cathode.

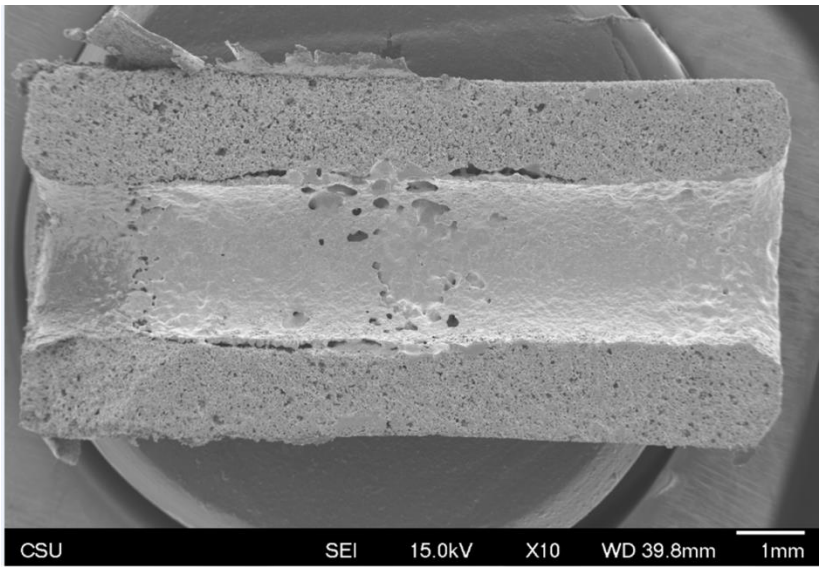

Fig. 20. SEM image of the cross sectioned and ion polished cermet insert removed from the Tubular 3 cathode after testing on Ar and iodine for 2.3 hr and 25 hr, respectively.

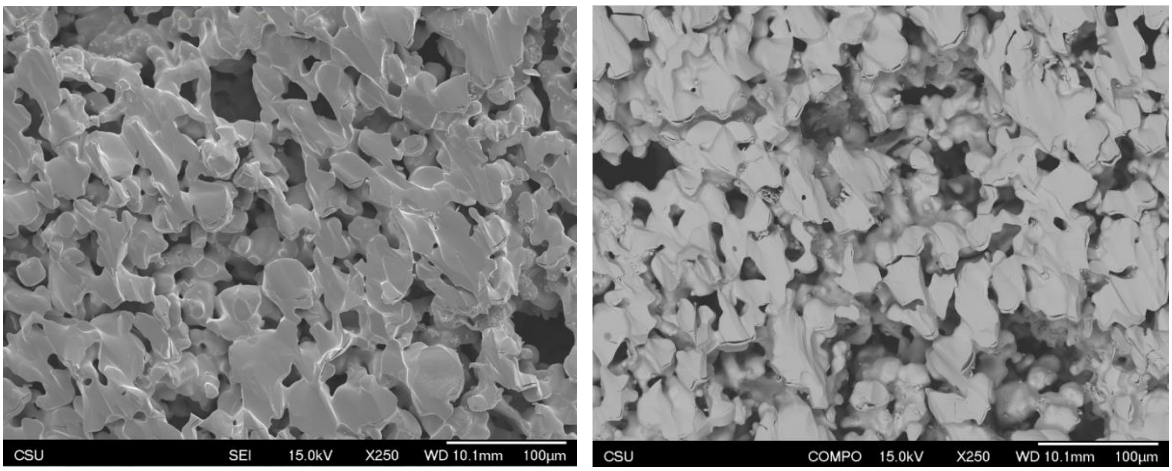

Fig. 21. SEM SEI and Compo images of the cermet insert removed from the Tubular 3 cathode after testing on Ar and iodine for 2.3 hr and 25 hr, respectively. Image was taken at an axially location of 0.5 mm upstream of the tip at a radial location midway between the inner and outer diameter. It was observed that the ceramic component of the cermet is nearly entirely removed leaving behind a foam-like interior, which would not conduct heat as well as a more solid, ceramic filled cermet would.

4. Details related to Tubular 4 cathode analysis

Several interesting observations were made after testing the Tubular 4 cathode on iodine for 22 hr. Recall that the insert in Tubular 4 was fabricated with 5:1 W to BCA ratio by weight similar to Tubular 1 and 2 and the Planar cermets. The Tubular 4 test was stopped by an interlock that tripped when the cooling water flow rate dropped below its minimum setting. Photographs of the Tubular 4 cathode with the modified keeper assembly are shown in Fig. 22, and SEM images of the cermet insert are shown in Figs. 23-27. The captions on the figures contain additional information about this cathode assembly that were different than Tubular 2 and 3 cathodes. We also note that a minor leak in the Ar feed system was eliminated before testing the Tubular 4 cathode.

Figure 24 shows that a significant amount of ceramic material still remains in the cermet at an axial location of 0.5 mm from the tip. Figure 25 conversely shows nearly no ceramic to exist at 1.0 mm upstream of the tip. Figure 26 contains images of the region ~6.5 mm upstream where sharp W crystals are forming. And finally Fig. 27 contrasts the Tubular 4 cermet at 0.5 mm with images of the Tubular 3 cermet at the same location. The caption

contains a list of interesting points about these two cermets that were both operated for similar times. We point out that the Tubular 4 cathode was operated at a lower iodine flow, and this lower flow might have caused it to operate in the plume mode.

Fig. 22. Photograph of the Tubular 4 cathode assembly before testing (left) and after testing (right). Note the deposits that formed on the anode just downstream of the keeper tip. The keeper tip was fabricated with a cap that could be removed to allow different keeper orifice plates to be used. The keeper ID was reduced and the cathode tip to keeper orifice plate distance was increased in an attempt to reduce arcing at startup on Ar.

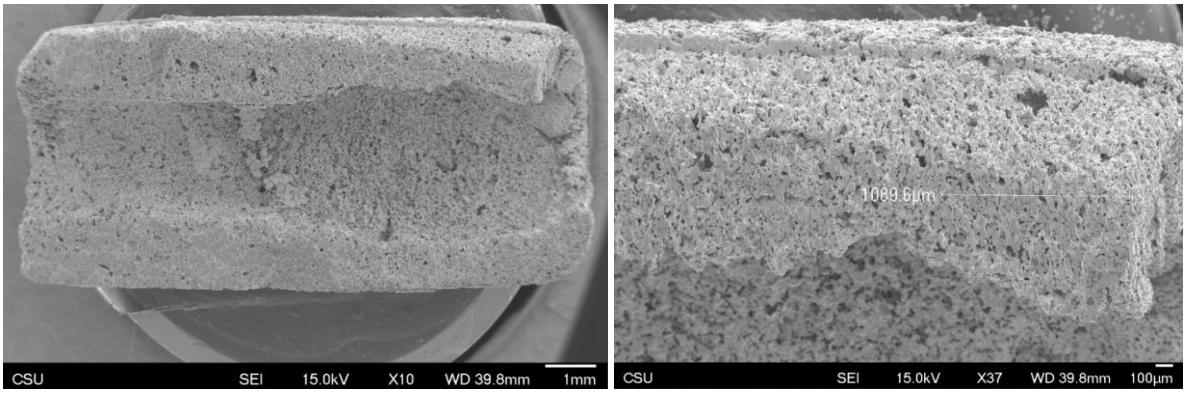

Figure 23. SEM images of the Tubular 4 cermet insert. Note the relatively large amount of erosion that occurred on the ID of the insert from the tip location to about 6 mm upstream. Note also the deposits that formed just upstream of 6 mm. The data presented in Figures 24-27 focus in on axial locations of 0.5 and 1.0 mm and on the features ~6 mm upstream of the tip.

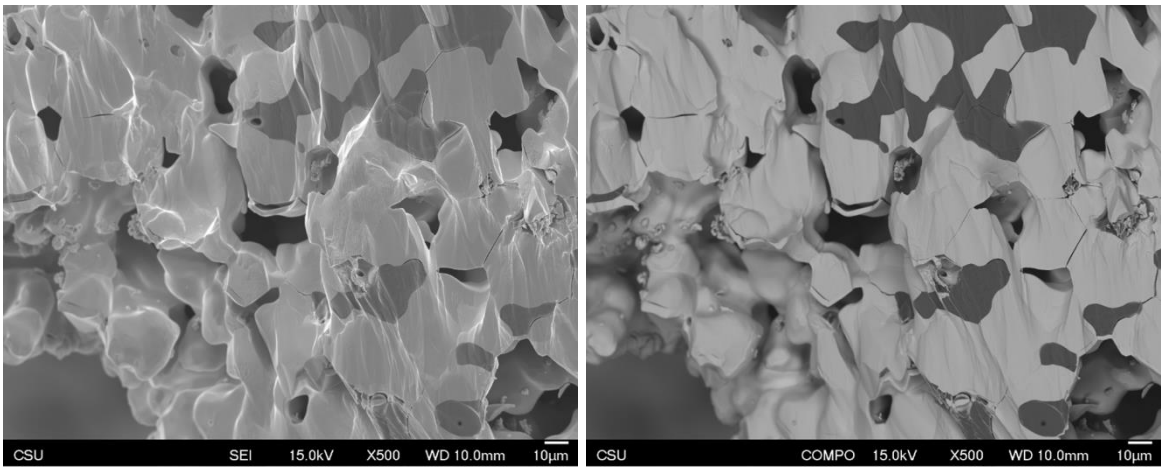

0.5 mm axial location, radially near ID

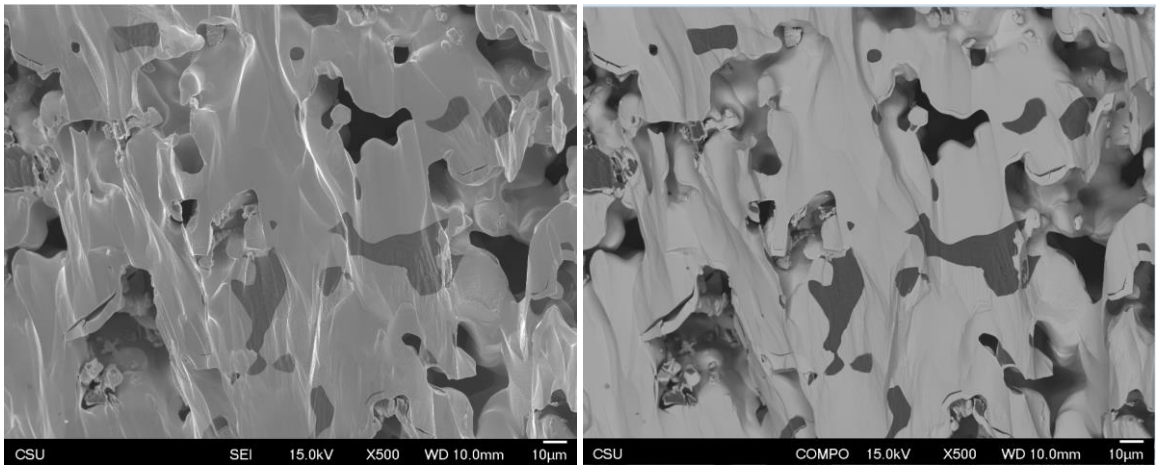

0.5 mm axial location, radially near the mid point of the wall

Figure 24. SEM SEI and Compo images of the Tubular 4 cermet insert.

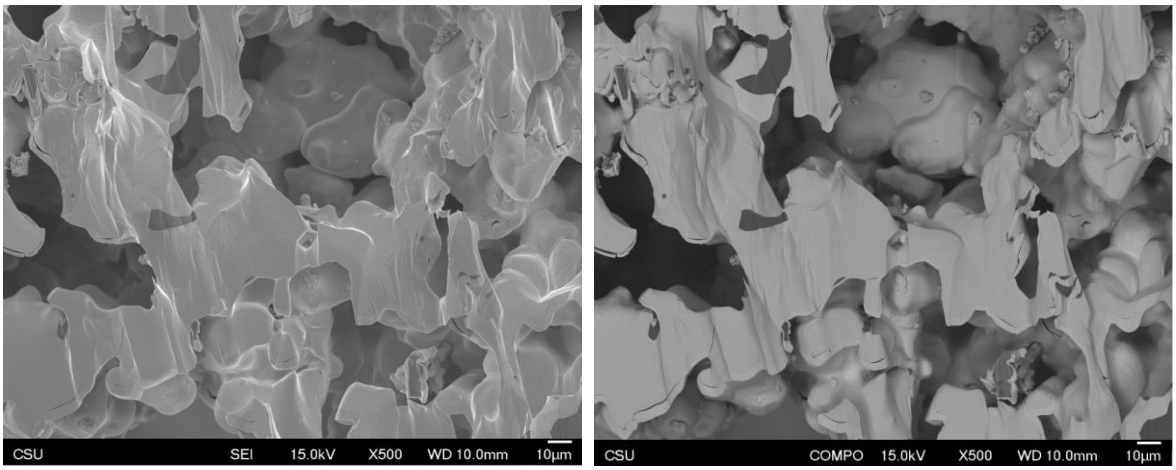

1.0 mm near ID

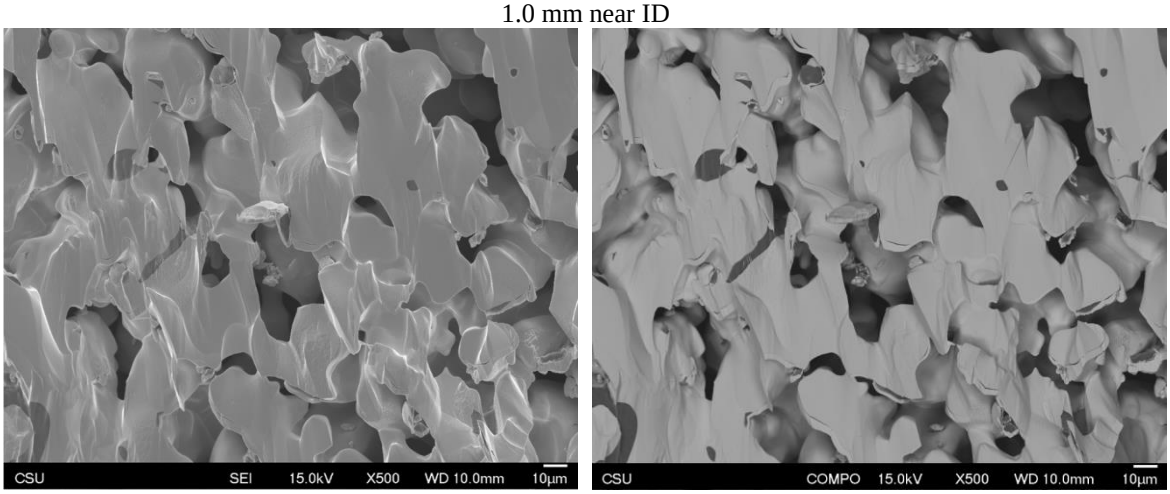

1.0 mm near mid wall

Figure 25. SEM SEI and Compo images of the Tubular 4 cermet insert.

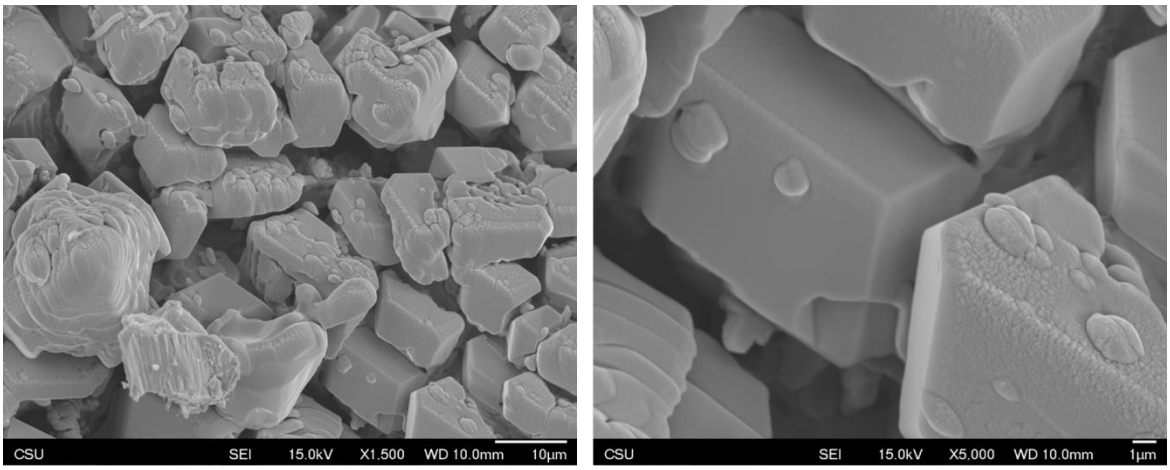

Figure 26. SEM SEI images of the Tubular 4 cermet insert at 6.5 mm upstream on the ID.

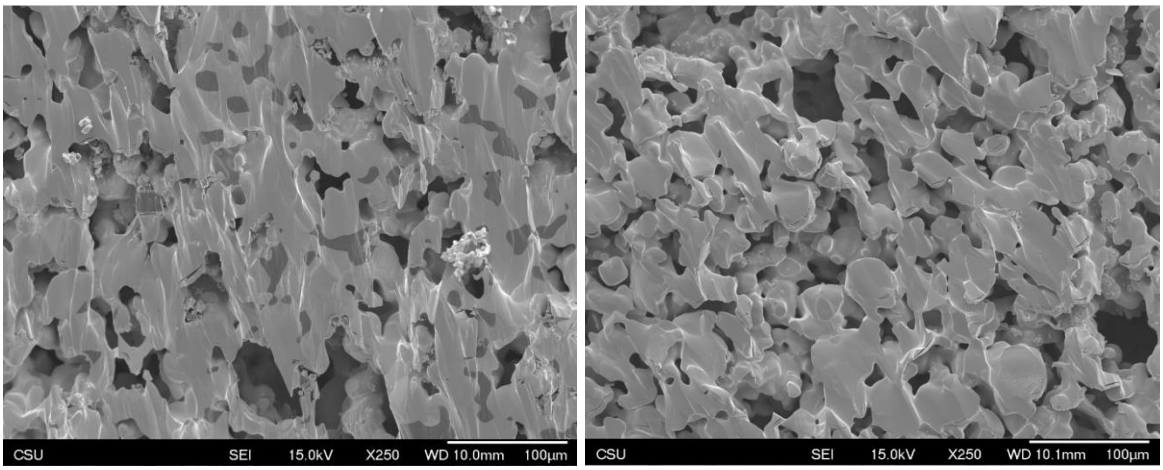

Tubular 4 Tubular 3

Fig. 27. Comparison of Tubular 4 and 3 inserts at the same location (axial 0.5 mm, radial near midwall). These inserts had different starting amounts of W relative to BCA. More ceramic was observed to be left over in the Tubular 04 insert at 0.5 mm, but very little was detected further upstream at 1.0 mm. Crystals formed on the interior of the Tubular 04 insert at ~6.5 mm. Compare to Fig. 14 of the Tubular 2 cermet (image on top left, which shows much less ceramic even though Tubular 2 was operated for less time than the Tubular 4 cathode. It is noted that Tubular 4 was operated at lower flow rates compared to the Tubular 2 and 3 cathodes.

5. Details related to Tubular 1 cathode analysis

We did not cross section Tubular 1 cathode or image the cathode insert as much as the other inserts discussed in this paper, but we did collect images of the inside surface of the insert near the tip region. These images are shown in Fig. 28. Very sharp-edged crystals formed inside the Tubular 1 insert whose radii of curvatures were smaller than the 10 nm resolution of the SEM. It is possible that these sharp features might emit electrons via tunneling that would lower the effective work function of the surface.

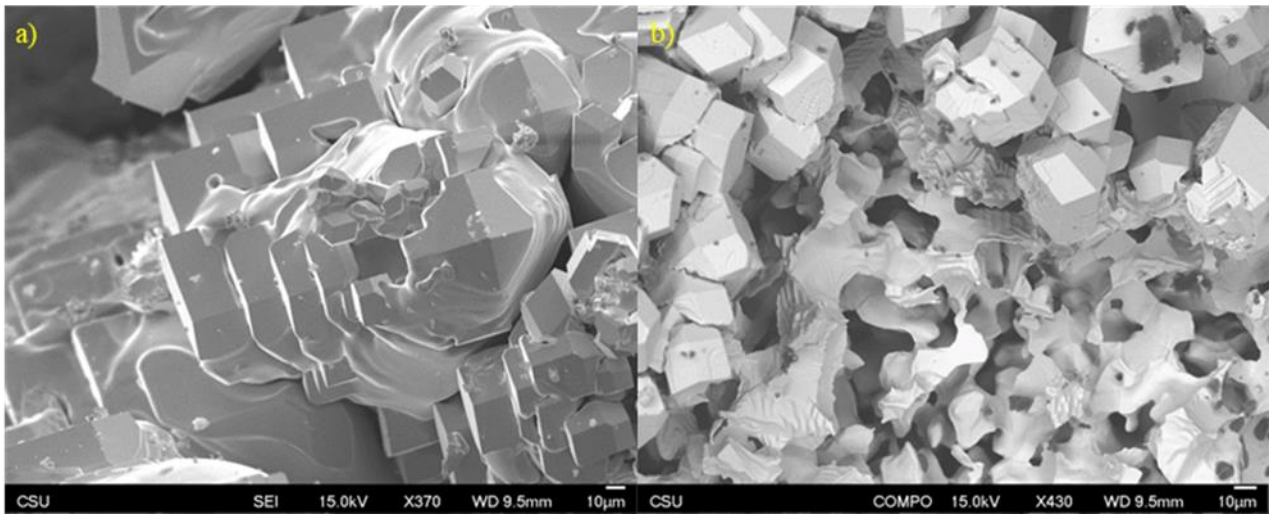

Fig. 28. Scanning electron microscope images of tubular 1 cathode insert after operation on iodine. The secondary electron image a) shows the formation of sharp edge block-like tungsten crystals. The composition image b) of a nearby region shows a porous tungsten foam structure that is largely void of ceramic.

V. Conclusion

A. Current Findings

Results with graphite cathodes containing a precursor cermet insert are encouraging. Very little to no signs of corrosion were observed inside the graphite cathode tube, therein confirming our expectation that carbon is a compatible material with iodine. The primary concern of using the graphite tube is the orifice wear observed after multiple cold starts of the cathode. The planar cathode that utilized a graphite plate in contact with the insert also showed little degradation over the 17 hours of operation on iodine, and due to its configuration could be adjusted to account for wear if present at low erosion rates.

Although changes, such as the mass transport of the ceramic insert materials out of the cathode orifice, were expected, the self-assembly formation of sharp tungsten points on the inside of the tubular insert material was not. The edges of these features are small enough that they could significantly enhance electric fields that may induce field emission aiding electron emission and effectively lowering the temperature required to emit electrons in a solely thermionic manner.

The removal of the ceramic material from the cermet insert results in the formation of a W foam-like material that would have reduced thermal conductivity relative to a cermet material filled with ceramic material. The lower thermal conductivity would likely result in higher insert temperatures, which, if elevated enough, might result in little to no iodine-induced erosion.

B. Recommendations for Future Work

As mentioned previously, the increased wear at the orifice of the graphite-based cathode tubes can raise concerns about cycle-life of the cathodes. As a result, a soft-start circuit is being developed to limit the damage of arcing events near the cathode orifice at startup of a heaterless hollow cathode. We are also investigating the effects of cermet and cathode geometry that might prevent cathodic arc formation during the start-up process. If these objectives could be achieved, graphite-based cathode tubes could be considered for use in long-lifetime iodine compatible hollow cathodes.

Future work will also include longer wear tests, and repeated, iodine-only start tests to confirm suitable on-off cycling capability for space missions of any kind. Current testing focuses on shorter tests of prototypes to identify important life-limiting mechanisms. In addition, accurate and reliable feed systems capable of providing real-time flow rate measurements based on measurements of iodine tank mass are being designed. This capability will enable cathode performance mapping to be conducted before, during, and after wear testing. Finally, we are currently developing a corrosion and erosion model of materials exposed to iodine at elevated temperatures that would serve as a tool to aid in cathode design.

Acknowledgments

The authors thank NASA for financially supporting this work under NASA SBIR Ph. 2 contract # NNX17CC71P. We would like to thank Dr. Gabriel F. Benavides of NASA GRC for his guidance in developing iodine testing facilities at Colorado State University. We would also like to thank Dr. Kurt Pulzin and Mr. John Dankanich of NASA MSFC for assisting SJT in testing many early prototype iodine hollow cathodes that enabled this work to unfold.

References

[1] J. Szabo, M. Robin, S. Paintal, B. Pote, V. Hruby, and C. Freeman, “Iodine plasma propulsion test results at 1-10 kW,” IEEE Trans. Plasma Sci., vol. 43, no. 1, pp. 141–148, 2015.
[2] J. Szabo et al., “Performance Evaluation of an Iodine-Vapor Hall Thruster,” J. Propuls. Power, vol. 28, no. 4, pp. 848–857, 2012.
[3] J. Szabo, M. Robin, S. Paintal, B. Pote, and V. Hruby, “High Density Hall Thruster Propellant Investigations,” in 48th AIAA/ASME/SAE/ASEE Joint Propulsion Conference & Exhibit, 2012, no. August, pp. 1–15.
[4] L. P. Rand and J. D. Williams, “Instant Start Electride Hollow Cathode,” in 33rd International Electric Propulsion Conference, 2013, pp. 1–11.
[5] D. M. Goebel and I. Katz, Fundamentals of Electric Propulsion: Ion and Hall Thrusters. 2008.

[6] D. M. Goebel, J. T. Crow, and A. T. Forrester, “Lanthanum hexaboride hollow cathode for dense plasma production,” Rev. Sci. Instrum., vol. 49, no. 4, pp. 469–472, 1978.
[7] W. L. Ohlinger, B. Vancil, and J. E. Polk, “Advanced Dispenser-Type Cathode Development for Electric Propulsion,” 52nd AIAA/SAE/ASEE Jt. Propuls. Conf., pp. 1–9, 2016.
[8] K. A. Polzin et al., “Propulsion System Development for the Iodine Satellite (iSAT) Demonstration Mission,” in Joint Conference of 30th International Symposium on Space Technology and Science, 34th International Electric Propulsion Conference and 6th Nano-satellite Symposium, 2015, pp. 1–14.
[9] C. B. Collins and E. G. Zubler, “Iodine Cycle Incandescent Lamps,” US 2883571 A, 1959.
[10] E. G. Fridrich and E. H. Wiley, “Electric Incandescent Lamp,” US 3132278 A, 1964.
[11] Ham, R. K., Williams, J. D., Hall, S. J., Benavides, G. F., and Verhey, T. R., “Characterization of Propellant Flow and Bias Required to Initiate an Arc Discharge in a Heaterless Hollow Cathode,” *Energy and Propulsion /Forum 2019*, Indianapolis, Indiana, American Institute of Aeronautics and Astronautics, 2019.
[12] Andreano, T.M., Williams, J.D., Clement, M., and Farnell, C.C., "Performance Comparison of a 1.5 kW Hall Thruster with Center-Mounted and Outer-Pole-Mounted Heaterless Cathodes," Energy and Propulsion Forum 2019, Indianapolis, Indiana, American Institute of Aeronautics and Astronautics, 2019.